

Joint Information Extraction with Cross-Task and Cross-Instance High-Order Modeling

Zixia Jia[‡], Zhaohui Yan[‡], Wenjuan Han[◇], Zilong Zheng[◇], Kewei Tu[‡]

[‡]School of Information Science and Technology, ShanghaiTech University

[◇]Beijing Institute for General Artificial Intelligence

{yanzh, jiazx, tukw}@shanghaitech.edu.cn

{hanwenjuan, zlzheng}@bigai.ai

Abstract

Prior works on Information Extraction (IE) typically predict different tasks and instances (e.g., event triggers, entities, roles, relations) independently, while neglecting their interactions and leading to model inefficiency. In this work, we introduce a joint IE framework, HighIE, that learns and predicts multiple IE tasks by integrating high-order cross-task and cross-instance dependencies. Specifically, we design two categories of high-order factors: homogeneous factors and heterogeneous factors. Then, these factors are utilized to jointly predict labels of all instances. To address the intractability problem of exact high-order inference, we incorporate a high-order neural decoder that is unfolded from a mean-field variational inference method. The experimental results show that our approach achieves consistent improvements on three IE tasks compared with our baseline and prior work.¹

1 Introduction

Information extraction (IE) has long been considered a fundamental challenge for various downstream natural language understanding tasks, such as knowledge graph construction, reading comprehension, and explainable question-answering systems, *etc.* The goal is to identify and extract structured information from unstructured natural language text, such that both users and machines can easily comprehend the entities, relations and events within the text.

Conventional IE schemes commonly suffer from two main problems. First, most approaches treat different IE tasks separately, while neglecting *cross-task dependencies*. Such isolated learning schemes lead to severely insufficient knowledge capturing and inefficient model constructions. Intuitively and empirically, predictions in different IE tasks can

¹The code and trained models can be found at <https://github.com/JZXXX/High-order-IE>.

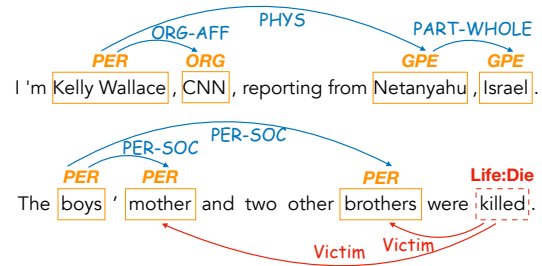


Figure 1: Example annotations of entity recognition (e.g., **PER**), relation extraction (e.g., **PER-SOC**) and event extraction tasks (e.g., **Life:Die** and **Victim**).

influence each other: types of entities can provide information that is useful to predict their relations or limit the roles they play in some events; a relation between two entities would restrict the types of the entities. For example in Figure 1, two entities linked by a **PART-WHOLE** relation are more likely to share the same entity types; the knowledge of event **Life:Die** and entity **PER** can benefit the prediction of the role **Victim**.

Second, although recent success has demonstrated significant improvements by utilizing cross-task information with multi-task learning scheme, the prediction methods are solely based on local classifiers while not considering the *cross-instance interactions* (e.g., event triggers, entities, roles, relations). For example, Luan et al. (2018) propose to use shared encoders with multi-task learning; Luan et al. (2019a); Wadden et al. (2019) update shared span representations according to local task-specific predictions; Lin et al. (2020a) design templates to generate global features as constraints in the training process. These works, however, only leverage interactions at the feature level and do not *explicitly* model the correlations between different instances and utilize them in inference. Some recent works study joint inference of different IE tasks (especially on joint entity and relation extraction) or integration of logic rules within neural network to constrain decoding (Wang and Pan, 2020, 2021). However, these methods are designed for

specific IE settings and hard to be generalized to other tasks.

Considering aforementioned two significant limitations, we propose a novel joint IE framework, **High-Order Information Extraction (HighIE)**, that *explicitly* models interactions across IE tasks and instances by high-order interactions. The term “high-order” in this work typically refers to scoring factors connecting two or more correlated instances in the same or across different tasks.

Specifically, we demonstrate the effectiveness of our proposed high-order framework on three widely-explored IE tasks: entity recognition (EntR), relation extraction (ReIE) and event extraction (EventE). To model the joint interactions between these tasks, we design two categories of high-order factors: **homogeneous factors (homo)** representing correlations between instances of the same task, and **heterogeneous factors (hete)** representing correlations between instances of different tasks. Taking EntR and EventE as an example, we calculate correlation scores of role-role pairs (homo), and trigger-role-entity triples (hete). We leverage these scores to jointly predict the labels of all instances. Since exact high-order inference is analytically intractable, we incorporate a neural decoder that is unfolded from the approximate mean-field variational inference method.

We highlight the main benefits and contributions of HighIE. First and the most straightforward, HighIE achieves better performance on individual IE tasks compared with previous state-of-the-art models. Second, we design two categories of high-order factors that can incorporate cross-task and cross-instance interactions both in training and inference processes. Third, our proposed high-order framework can be easily generalized to any other span-relation graph prediction tasks, such as frame semantic parsing and opinion role labeling.

2 High-Order Information Extraction

2.1 Joint IE as Graph Prediction

We investigate three widely-explored IE tasks.

- ▷ EntR aims to identify some spans in a sentence as entities and label their entity types.
- ▷ ReIE aims to identify relations between some entity pairs and label their relation types.
- ▷ EventE aims to label event types and its trigger words, identify some entities as event arguments and label argument roles.

We formulate the three IE tasks as a graph $G =$

(V, E) prediction task, where V denotes the node set representing predicted text entities or triggers and E denotes the directed edge set representing nodes’ dependencies. Each node $v = (a, b, l) \in V$ is a span for a trigger or an entity, where a and b index the start and end words of the span, and $l \in \mathcal{L}^{\text{event}}$ or $l \in \mathcal{L}^{\text{entity}}$ denotes the node’s event type and entity type, respectively. Each edge $e_{ij} = (i, j, r) \in E$ represents the relationship between a node pair, where i and j index the head and tail nodes, and $r \in \mathcal{R}^{\text{role}}$ or $r \in \mathcal{R}^{\text{relation}}$ represents the edge label which is a role type when the edge is from a trigger to an entity (as an argument) or a relation type when the edge is from one entity to another.

Figure 2(A) depicts the overall architecture of HighIE. Because joint identification and classification need to enumerate all possible spans as nodes and the high-order inference whose complexity is related to the node number becomes too computationally expensive in this situation, we first use a node identification module to identify spans in the input sentence as graph nodes. Then, we design a classification module to predict (i) a label for each node and (ii) a label for the edge between each node pair, where we use a special NULL label to represent the non-existence of an edge. Our classification module incorporates cross-instance (*e.g.*, a pair of relations on ReIE) and cross-task (*e.g.*, EntR and EventE) correlations by designing homogeneous and heterogeneous high-order factors. Note that the classification module requires identified nodes as input, so we train the node identification module first and then fix it during subsequent training of the classification module.

Node Identification Module Following previous work (Lample et al., 2016a; Lin et al., 2020a), we formulate node identification as a sequence labeling task with a BIO scheme. For word features, we adopt a pre-trained transformer-based encoder, such as BERT (Devlin et al., 2018). We use the average of all sub-word embeddings extracted from the encoder as the word representation. The decoder is formulated as a vanilla linear-chain conditional random field (CRF) (Lafferty et al., 2001). Specifically, we use Viterbi algorithm (Forney, 1973) to obtain a sequence with the highest score, then select the spans whose inter-words are labeled as B-X and I-X in the optimal output sequence as predicted node set. More details can be found in Appendix A. Following previous work,

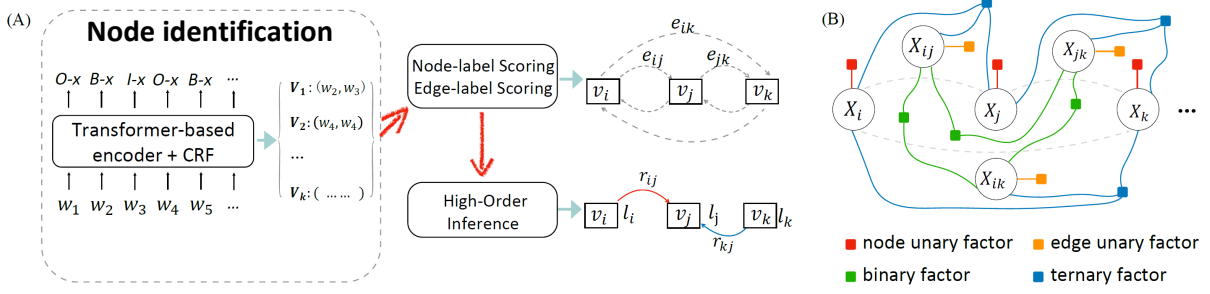


Figure 2: **An overview of HighIE.** (A) Model architecture. The identification module provides spans as nodes to the classification module. (B) An example factor graph of our classification module containing variables representing three nodes and three edges. X_i indicates the label variable of the i -th node and X_{ij} indicates the label variable of the edge from the i -th node to j -th node. The node labels can be event types or entity types. The edge labels can be relations or argument roles. For simpler illustration, we omit edges of the opposite direction.

we did not consider nested spans in this work.

Classification Module Instead of predicting each node and edge independently with a local classifier, the classification module predicts node labels and edge labels with high-order interactions and joint inference. We describe our high-order classification module in following subsections.

2.2 High-Order Modeling

Figure 2(B) illustrates the factor graph underlying our classification module. Typically, we design three categories of factors: unary factors that reflect the likelihood distribution of each variable’s label; binary factors for a pair of edges sharing the same endpoint; and ternary factors for an edge, its head node and its tail node. The potential function of a factor is defined as the exponential of the corresponding scores, *i.e.*, $\phi(X) = \exp(s_X)$. We discuss the detailed scoring functions as follows.

Unary Scoring We first obtain each node’s representation \mathbf{z} by averaging the representations of all the words within the predicted span, in which the words’ representations are obtained in the same way as in the identification module. Then, the unary scores of the i -th node labels $\mathbf{s}_i^{u-ntask} \in \mathbb{R}^{|L^{ntask}|}$ can be obtained by feeding \mathbf{z}_i into a two layers task-specific feed-forward neural network (FNN):

$$\mathbf{s}_i^{u-ntask} = \text{FNN}^{ntask}(\mathbf{z}_i), \quad (1)$$

where L^{ntask} represents a task-specific node label set, and $ntask \in \{\text{event}, \text{entity}\}$.

The unary label scores $\mathbf{s}_{ij}^{u-etask}$ of an edge e_{ij} from the i -th node to the j -th node can be computed with a decomposed biaffine function:

$$\mathbf{s}_{ij}^{u-etask} = (\text{FNN}^{etask-s}(\mathbf{z}_i) \circ \text{FNN}^{etask-e}(\mathbf{z}_j)) \mathbf{H}^{u-etask} \quad (2)$$

where two $\text{FNN}(\cdot)$ denote task-specific single-layer FNNs, $\mathbf{H}^{u-etask} \in \mathbb{R}^{d_2 \times |\mathcal{R}^{etask}|}$ is a trainable matrix with random initialization, \mathcal{R}^{etask} represents a task-specific edge label set that includes an additional $\langle \text{NULL} \rangle$ label, $etask \in \{\text{relation}, \text{role}\}$, and \circ denotes element-wise product.

Binary Scoring We calculate binary correlation scores of each edge pair that share one endpoint. As illustrated in Figure 2(A), there are three types of binary factors (Wang et al., 2019b): edge e_{ij} and edge e_{ik} share the head node v_i , producing sibling (sib); edge e_{jk} and edge e_{ik} share the tail node v_k , producing co-parent (cop); and the tail node v_j of edge e_{ij} is the head node of edge e_{jk} , producing grandparent (gp). For each specific type of binary factors, we use different single-layer FNNs taking \mathbf{z} as input to calculate a head representation (-s) and a tail representation (-e) for each node. For gp factor, we additionally calculate a middle representation (-mid) for each node.

$$\begin{aligned} \mathbf{g}_i^{type-s} &= \text{FNN}^{type-s}(\mathbf{z}_i) & \mathbf{g}_i^{type-e} &= \text{FNN}^{type-e}(\mathbf{z}_i) \\ \mathbf{g}_i^{type-mid} &= \text{FNN}^{type-m}(\mathbf{z}_i) & type &\in \{\text{sib}, \text{cop}, \text{gp}\} \end{aligned}$$

For a sib pair $\{e_{ij}, e_{ik}\}$, cop pair $\{e_{ik}, e_{jk}\}$ and gp pair $\{e_{ij}, e_{jk}\}$, suppose that the first edge has label $m \in \mathcal{R}^1$ and the second edge has label $n \in \mathcal{R}^2$, we formulate binary scores as follows:

$$\begin{aligned} s_{ijkmn}^{\text{sib}} &\equiv s_{ikjnm}^{\text{sib}} \\ &= \sum_{a=1}^{d_3} (\mathbf{g}_i^{\text{sib-s}} \circ \mathbf{g}_j^{\text{sib-e}} \circ \mathbf{g}_k^{\text{sib-e}} \circ \mathbf{h}_m^1 \circ \mathbf{h}_n^2)_a \\ s_{ijkmn}^{\text{cop}} &\equiv s_{ikjnm}^{\text{cop}} \\ &= \sum_{a=1}^{d_3} (\mathbf{g}_i^{\text{cop-s}} \circ \mathbf{g}_j^{\text{cop-s}} \circ \mathbf{g}_k^{\text{cop-e}} \circ \mathbf{h}_m^1 \circ \mathbf{h}_n^2)_a \\ s_{ijkmn}^{\text{gp}} &= \sum_{a=1}^{d_3} (\mathbf{g}_i^{\text{gp-s}} \circ \mathbf{g}_j^{\text{gp-mid}} \circ \mathbf{g}_k^{\text{gp-e}} \circ \mathbf{h}_m^1 \circ \mathbf{h}_n^2)_a \end{aligned}$$

where \mathbf{h}_m^1 is the embedding of the first edge label m and \mathbf{h}_n^2 is the embedding of the second edge label n . Both \mathbf{g} and \mathbf{h} are d_3 -dimensional.

In this paper, we consider two types of homogeneous binary factors: **case (i)** sib and cop representing two argument roles ($\mathcal{R}^1 = \mathcal{R}^2 = \mathcal{R}^{\text{role}}$) and **case (ii)** sib, cop and gp representing two relations ($\mathcal{R}^1 = \mathcal{R}^2 = \mathcal{R}^{\text{relation}}$). We also consider one type of heterogeneous binary factors: **case (iii)** cop and gp where one edge label is a relation and the other is a role for joint EventE and RelE ($\mathcal{R}^1 = \mathcal{R}^{\text{relation}}, \mathcal{R}^2 = \mathcal{R}^{\text{role}}$ or $\mathcal{R}^1 = \mathcal{R}^{\text{role}}, \mathcal{R}^2 = \mathcal{R}^{\text{relation}}$).²

Ternary Scoring We calculate ternary correlation scores of an edge and its two endpoints. Figure 2(B) illustrates ternary factors. Similar to binary scoring, we use two new FNNs to produce representations for each possible head node and tail node respectively.

$$\mathbf{g}_i^{\text{ter-s}} = \text{FNN}^{\text{ter-s}}(\mathbf{z}_i) \quad \mathbf{g}_i^{\text{ter-e}} = \text{FNN}^{\text{ter-e}}(\mathbf{z}_i)$$

For an edge with label $m \in \mathcal{R}$, its head node v_i having label $p \in \mathcal{L}^s$ and its tail node v_j having label $q \in \mathcal{L}^e$, the ternary score can be calculated as:

$$s_{ijpqm}^{\text{ter}} = \sum_{a=1}^{d_4} (\mathbf{g}_i^{\text{ter-s}} \circ \mathbf{g}_j^{\text{ter-e}} \circ \mathbf{e}_p^{\text{ter-s}} \circ \mathbf{e}_q^{\text{ter-e}} \circ \mathbf{h}_m^{\text{ter}})_a \quad (3)$$

where $\mathbf{h}_m^{\text{ter}}$ is the embedding of label m , $\mathbf{e}_p^{\text{ter-s}}$ is the embedding of label p and $\mathbf{e}_q^{\text{ter-e}}$ is the embedding of label q . \mathbf{g} , \mathbf{e} and \mathbf{h} are all d_4 -dimensional. We consider two types of heterogeneous ternary factors: the ternary correlations between **case (i)** an event, an entity (as a possible argument), and a role between them for joint EventE and EntR ($\mathcal{L}^s = \mathcal{L}^{\text{event}}, \mathcal{R} = \mathcal{R}^{\text{role}}$ and $\mathcal{L}^e = \mathcal{L}^{\text{entity}}$) and **case (ii)** two entities and a relation between them for joint RelE and EntR ($\mathcal{L}^s = \mathcal{L}^e = \mathcal{L}^{\text{entity}}$ and $\mathcal{R} = \mathcal{R}^{\text{relation}}$).

2.3 High-Order Inference

In contrast to the first-order inference which independently predicts the value of each variable by maximizing its unary score, in high-order inference we jointly predict the values of all the variables to maximize the sum of their unary and

²It is rare that a trigger word serves as an argument meanwhile, and a relation edge and a role edge cannot share the same head node, so we do not consider gp in case (i) and sib in case (iii).

high-order scores. However, the exact joint inference on our factor graph is NP-hard in general. Therefore, we use Mean-Field Variational Inference (MFVI) (Xing et al., 2012) for approximate inference. MFVI iteratively updates an approximate posterior marginal distribution $Q(X)$ of each variable X based on messages from all the factors connected to it. Messages for edge variables aggregated from binary factors are calculated as:

$$\begin{aligned} & F_{\text{bi}}^{(t-1)}(X_{ij} = m) \\ &= \sum_{k \neq i, j} \sum_{n \in \mathcal{R}^2} \alpha_1 \times s_{ijkmn}^{\text{sib}} \times Q_{ik}^{(t-1)}(X_{ik} = n) + \\ & \quad \alpha_2 \times s_{ikjmn}^{\text{cop}} \times Q_{kj}^{(t-1)}(X_{kj} = n) + \\ & \quad \alpha_3 \times (s_{ijkmn}^{\text{gp}} \times Q_{jk}^{(t-1)}(X_{jk} = n) + \\ & \quad \quad s_{kijmn}^{\text{gp}} \times Q_{ki}^{(t-1)}(X_{ki} = n)) \end{aligned}$$

where $\alpha_1, \alpha_2, \alpha_3 \in [0, 1]$ are hyper-parameters controlling the scale of messages passed by the different types of binary factors. These hyper-parameters are not part of standard MFVI and can instead be seen as part of the scoring function.

Messages for node variables and edge variables aggregated from ternary factors are calculated as:

$$\begin{aligned} F_{\text{ter}}^{(t-1)}(X_{ij} = m) &= \sum_{p \in \mathcal{L}^s} \sum_{q \in \mathcal{L}^e} s_{ijpqm}^{\text{ter}} \\ & \quad \times Q_i^{(t-1)}(X_i = p) \times Q_j^{(t-1)}(X_j = q) \\ F_{\text{ter}}^{(t-1)}(X_i = p) &= \sum_{q \in \mathcal{L}^e} \sum_{m \in \mathcal{R}} s_{ijpqm}^{\text{ter}} \\ & \quad \times Q_j^{(t-1)}(X_j = q) \times Q_{ij}^{(t-1)}(X_{ij} = m) \\ F_{\text{ter}}^{(t-1)}(X_j = q) &= \sum_{p \in \mathcal{L}^s} \sum_{m \in \mathcal{R}} s_{ijpqm}^{\text{ter}} \\ & \quad \times Q_i^{(t-1)}(X_i = p) \times Q_{ij}^{(t-1)}(X_{ij} = m) \end{aligned}$$

The posterior $Q(X)$ is updated based on the messages as follows:

$$\begin{aligned} Q_{ij}^{(t)}(X_{ij} = m) &\propto \exp\{s_{ijm}^{\text{u-etask}} \\ & \quad + \alpha_4 F_{\text{bi}}^{(t-1)}(X_{ij} = m) + \alpha_5 F_{\text{ter}}^{(t-1)}(X_{ij} = m)\} \\ Q_i^{(t)}(X_i = p) &\propto \exp\{s_{ip}^{\text{u-ntask}} + \alpha_6 F_{\text{ter}}^{(t-1)}(X_i = p)\} \\ Q_j^{(t)}(X_j = q) &\propto \exp\{s_{jq}^{\text{u-ntask}} + \alpha_7 F_{\text{ter}}^{(t-1)}(X_j = q)\} \end{aligned}$$

where all $\alpha \in [0, 1]$ are hyper-parameters controlling the scale of different types of messages, $s_{ijm}^{\text{u-etask}}$ is the m -th element of $s_{ij}^{\text{u-etask}}$ in Eq. 2, $s_{ip}^{\text{u-ntask}}$ is the p -th element of $s_i^{\text{u-ntask}}$ and $s_{jq}^{\text{u-ntask}}$ is the q -th element of $s_j^{\text{u-ntask}}$ in Eq. 1.

There are two ways of iterative MFVI update. In the synchronous update, we update $Q(X)$ for all the variables at each step. In asynchronous update, we alternate between node variables and edge variables for $Q(X)$ update. We empirically find that asynchronous update is better than synchronous update when we use ternary factors in some cases.

Inspired by Zheng et al. (2015); Wang et al. (2019b), the iterative update steps can be unfolded as recurrent neural network layers parameterized by unary and high-order scores. The initial distribution $Q^{(0)}$ is set by normalizing exponentiated unary scores. After a fixed T (which is a hyper-parameter) number of iterations, we obtain the posterior distribution $Q^{(T)}$. For each variable, we choose the label that has the highest probability according to $Q^{(T)}$ as our prediction.

2.4 Multitask Training

Given a sentence $\mathbf{w} = (w_1, \dots, w_k)$, to train multiple IE tasks with our unified high-order span-relation prediction framework, we do multi-task learning with cross-entropy losses as follows:

$$\mathcal{L} = -\sum_i \log P(\hat{y}_i^{ntask} | \mathbf{w}) - \sum_{i,j} \log P(\hat{y}_{ij}^{etask} | \mathbf{w})$$

where \hat{y}_i^{ntask} and \hat{y}_{ij}^{etask} denote the ground truth labels of nodes and edges respectively for all the tasks. The conditional distributions over node labels and edge labels with first-order inference are

$$P(\mathbf{y}_i^{ntask} | \mathbf{w}) = \text{SoftMax}(\mathbf{s}_i^{u-ntask})$$

$$P(\mathbf{y}_{ij}^{etask} | \mathbf{w}) = \text{SoftMax}(\mathbf{s}_{ij}^{u-etask}),$$

and those with high-order inference are

$$P(y_i^{ntask} = X_i | \mathbf{w}) = Q_i^{(T)}(X_i)$$

$$P(y_{ij}^{etask} = X_{ij} | \mathbf{w}) = Q_{ij}^{(T)}(X_{ij}).$$

As such, the process of calculating posteriors in MFVI is fully differentiable and can be seen as a recurrent neural network. We are able to implement end-to-end training.

3 Experiments

Settings Because our framework models cross-task interactions with heterogeneous factors, each setting of our experiments contains at least two tasks (e.g., EntR and EventE, EntR and ReIE, all of them). Note that when we only use homogeneous factors in one task with high-order inference

(i.e., only cross-instance), the other tasks employ only first-order inference and are jointly trained as auxiliary tasks.

Datasets We evaluate our model on the ACE2005 corpus (Walker et al., 2005) which provides entity, relation, and event annotations. Following Lu et al. (2021a); Lin et al. (2020a); Wadden et al. (2019), we conduct experiments on three English datasets and one Chinese dataset: ACE05-R for EntR and ReIE, ACE05-E and ACE05-CN for EntR and EventE, and ACE05-E+ for all the three tasks, with the same data pre-processing and train/dev/test split. There are 7 entity types, 6 relation types, 33 event types, and 22 argument roles defined in these datasets. Detailed data statistics are provided in Appendix B.

Evaluation We use F1 scores to evaluate our model’s performance as in most previous work (Lu et al., 2021a; Lin et al., 2020a; Wadden et al., 2019). For the EntR task, an entity (*Ent*) is correct if both its type and offsets match a gold entity. For the ReIE task, a relation (*Rel*) is correct if both its type and the offsets of its two related entities match a gold relation. In addition, a strict relation evaluation (*Rel+*) requires that the types of the two related entities are also correct. A trigger is correctly identified (*Trig-I*) if its offsets match a gold trigger. It is correctly classified (*Trig-C*) if its corresponding event type also matches the reference trigger. An argument is correctly identified (*Arg-I*) if its offsets match a gold argument and its corresponding event type is correct. It is correctly classified (*Arg-C*) if its role type also matches the reference argument. All experimental results of our approach shown in this paper are the average of three runs with different random seeds.

Implementation Details For fair comparison with previous state-of-the-art systems, we use the BERT-large-cased model (Devlin et al., 2018) as our encoder for the ACE05-E and ACE05-E+ datasets, and ALBERT model (Lan et al., 2019) as the encoder for the ACE05-R dataset. We train our model with BertAdam optimizer³. α is set to 1 when a factor is used, and set to 0 otherwise. Detailed hyper-parameter values are provided in Appendix C.

³<https://github.com/huggingface/transformers>

	Ent	Tri-I	Tri-C	Arg-I	Arg-C
Wadden et al. (2019)	89.7	-	69.7	53.0	48.8
Zhang et al. (2019) ^o	87.1	73.9	72.0	57.2	52.4
Lin et al. (2020b)	90.2	78.2	74.7	59.2	56.8
Lin et al. (2020b) _{re-run}	90.9	77.1	73.6	58.7	56.4
Lu et al. (2021a) [*]	-	-	71.9	-	53.8
Our baseline	90.8	77.7	74.8	58.5	56.4
Our homo (+sib)	90.6	77.7	74.5	59.1	57.1
Our homo (+sib+cop)	90.8	77.7	74.6	58.7	57.1
Our hete (+ter)	90.7	77.7	74.8	59.2	56.9
Our hete (+sib+ter)	90.6	77.7	74.6	58.8	56.8

Table 1: Average F1 on ACE05-E dataset. Subscript *re-run* means the average result of our three re-runs using the code and config that the authors provide. To prove that our model achieves significantly better performance than previous work, we re-run the SOTO model and do a significant test based on Almost Stochastic Dominance (Dror et al., 2019). Scores being boldfaced means that they are significantly the best. ^o and ^{*} mean ELMo and T5-large encoder, respectively. *hete* and *homo* represent heterogeneous factors and homogeneous factors, respectively.

	Ent	Tri-C	Arg-I	Arg-C
Our baseline	96.0	93.1	70.7	68.3
Our homo (+sib)	96.0	93.6	72.0	69.2
Our hete (+ter)	95.9	94.1	71.7	69.2
Our hete (+sib+ter)	96.0	93.6	72.3	69.4

Table 2: Average F1 on ACE05-E dataset. The gold triggers and entities are given.

3.1 Main Results

We take our framework with first-order classification (i.e., independently predicting the value of each variable by maximizing its unary score) as **Our baseline**. We experiment with different combinations of tasks.

Joint EntR, EventE We compare our approach under different settings and also with previous work that did not leverage gold triggers and entities. Table 1 shows the experimental results. For our model, ***homo (+sib)+cop*** means that we use homogeneous sibling/coparent factors as described in the Binary Scoring case (i) of Sec 2.2, and ***hete (+ter)*** means that we use heterogeneous ternary factors as described in Ternary Scoring case (i) of Sec 2.2. ***hete (+sib+ter)*** means that we use both sibling factors and ternary factors at the same time. Note that the F1 scores of *Tri-I* of our model are the same in all the settings because they are produced by the same node identification module that is fixed to fairly compare our model in different settings.

It can be seen that our high-order model performs better than our baseline in most cases for EventE. Compared with previous SOTA on the

	Ent	Rel	Rel+
DYGIE++ [†] (Wadden et al., 2019)	88.6	63.4	-
OneIE [†] (Lin et al., 2020b)	88.8	67.5	-
Wang and Lu (2020) [‡]	89.5	67.6	64.3
PURE _s [‡] (Zhong and Chen, 2020)	89.7	69.0	65.6
UNIRE [‡] (Wang et al., 2021)	90.2	-	66.0
PFN [‡] (Yan et al., 2021)	89.0	-	66.8
UIE [*] (Lu et al., 2022)	-	-	66.1
Our baseline[‡]	89.8	69.9	67.5
Our homo (+sib)[‡]	90.0	70.8	68.1
Our homo (+cop)[‡]	90.1	70.1	68.0
Our homo (+gp)[‡]	90.2	70.0	67.7
Our homo (+sib+cop)[‡]	90.2	70.8	68.2
Our hete (+ter)[‡]	90.1	70.4	68.3
FOR REFERENCE			
PURE _c [‡] (Zhong and Chen, 2020)	90.9	69.4	67.0
PL-Marker _{re-eval} [‡] (Ye et al., 2022)	91.3	72.5	70.5

Table 3: Average F1 on ACE05-R dataset. Subscript of *re-eval* means re-evaluation (Appendix D) using the standard evaluation method as other work. ^{*} means the model uses T5-large, [†] means BERT-large-cased and [‡] means ALBERT-XXLarge-v1. PURE_s refers to the PURE model with single-sentence features. The results of PURE_c and PL-Marker are listed for reference because they use cross-sentence features and are not directly comparable with other models.

	Ent	Rel	Tri-I	Tri-C	Arg-I	Arg-C
Lin et al. (2020b)	89.6	58.6	75.6	72.8	57.3	54.8
Lin et al. (2020b) _{re}	90.8	65.2	76.5	73.7	59.6	57.3
Lu et al. (2021a) [*]	-	-	-	71.8	-	54.4
Lu et al. (2022) [*]	-	-	-	73.4	-	54.8
Liu et al. (2022)	-	-	-	74.3	-	54.7
Our baseline	90.8	65.3	77.4	74.6	60.0	58.1
Our hete (+cop)	90.7	65.9	77.4	74.6	60.3	58.2
Our hete (+gp)	90.7	65.8	77.4	75.1	60.8	59.0
Our hete (+cop+gp)	90.7	65.1	77.4	74.8	60.3	58.5

Table 4: Average F1 on ACE05-E+ dataset. Subscript *re* denotes the result of our re-implementation. ^{*} denotes T5-large.

EventE task, our baseline model can achieve comparable performance and our high-order model improves further. For EntR, our high-order models have similar performance to the baseline and previous SOTA. The reason is that only a small subset of entities participate in events as arguments, so most entities cannot receive helpful messages from event types or roles. We see that using both sibling and coparent factors has a similar performance to using only sibling factors, which shows that the interactions between two events that share the same argument are weak (the case is indeed scarce in the dataset, compared to sib). It is surprising that when we use both sibling factors and ternary factors (+sib+ter), the performance slightly drops. Since our high-order model focus on the classification process, we also evaluate our model given gold

	<i>Ent</i>	<i>Tri-I</i>	<i>Tri-C</i>	<i>Arg-I</i>	<i>Arg-C</i>
Lin et al. (2020b)	88.5	-	65.6	-	52.0
Our baseline	87.9	68.1	65.4	56.9	53.6
Our high-order	88.6	68.1	65.9	57.8	53.9

Table 5: Average F1 on ACE05-CN dataset. We adopt BERT-base-multilingual-cased encoder as Lin et al. (2020b).

triggers and entities to eliminate the impact of the identification module. Table 2 shows the experimental results. We can find that without the error of the identification module, the performance gap between our baseline and high-order models further increases, and using both sibling factors and ternary factors improves further.

As shown in Table 5, our model still achieves consistent improvement on the Chinese dataset.

Joint EntR and ReIE Table 3 shows our experimental results on the ACE05-R dataset, where *homo (+sib/+cop/+gp)* means homogeneous sibling/co-parent/grandparent factors as described in Binary Scoring case (ii) of Sec 2.2, and *hete (+ter)* means heterogeneous ternary factors as described in Ternary Scoring case (ii) of Sec 2.2. We can find that our high-order model performs better than most previous work and our baseline both on EntR and ReIE, which demonstrates the advantage of high-order inference. Similar to joint EntR and EventE, our high-order model with the combination of all factors cannot achieve further improvement, so we do not show the result of this setting.

Joint EntR, EventE and ReIE To test our heterogeneous binary factors as described in Binary Scoring case (iii) of Sec 2.2, we experiment with joint EntR, EventE and ReIE on the ACE05-E+ dataset. Table 4 shows the experimental results. Our high-order model with gp factors can be seen to perform the best. More experimental results on the ACE05-E+ can be found in Appendix E.

3.2 Analysis

High-Order Scoring We study two variants of our high-order scoring in Sec 2.2. *Share* means that we reuse the label representations in unary scoring for high-order scoring instead of using new label representations. *W/o node reps* means that we calculate high-order scores without taking node representations into account, such that the high-order scores are only dependent on the labels regardless of the underlying text spans that constituent the

	<i>Ent</i>	<i>Rel</i>	<i>Rel+</i>
Ours <i>hete (+ter)</i>	90.1	70.4	68.3
<i>Share</i>	90.0	69.7	67.5
<i>W/o node reps</i>	90.1	70.0	67.7

Table 6: Comparison of the results of different high-order scoring methods on ACE05-R dataset.

	<i>Ent</i>	<i>Tri-I</i>	<i>Tri-C</i>	<i>Arg-I</i>	<i>Arg-C</i>
<i>Asyn (+ter)</i> [†]	90.9	77.7	74.3	59.2	57.2
<i>Syn (+ter)</i> [†]	90.7	77.7	74.8	59.2	56.9

Table 7: Comparison of the results of synchronous and asynchronous updating strategies when we use ternary factor on ACE05-E dataset.

	<i>baseline</i>	<i>+sib</i>	<i>+ter</i>	<i>+sib+ter</i>
Train	119.3	119.2	118.4	107.6
Test	91.2	85.1	81.4	77.2

Table 8: Comparisons of training and testing speed (sentences/second) among the baseline model and high-order models on joint EntR, EventE and ReIE tasks.

nodes and edges. Table 6 shows the comparison results with ternary factors on the ACE05-R dataset. We can find that the performance of the two variants both drops.

Message Passing of Ternary Factors From the message passing process involving ternary factors in Sec. 2.3, we can see that messages passed to an edge come only from its two endpoints, but a node gets messages from all possible edges connected to it, which causes asymmetry messages from ternary factors, we try synchronous and asynchronous updating strategies as described in Sec 2.3. For asynchronous updating, we firstly update edge posteriors using node posteriors for the reason that the initial node posteriors are more accurate. Table 7 shows the comparison results of the two updating strategies on the ACE05-E dataset. We can find that asynchronous update has an advantage over synchronous update on *Arg-C* but harms the performance on *Tri-C*, which shows that asynchronous updating does benefit role prediction but may influence the trigger prediction.

Complexity and Speed of High-order Inference The computational complexity of our high-order inference is $O(n^3|\mathcal{R}|^2 + n|\mathcal{L}|)$ when we consider binary factors and $O(n^2|\mathcal{R}||\mathcal{L}|^2)$ when we consider ternary factors, while our first-order model has a computational complexity of $O(n^2|\mathcal{R}| + n|\mathcal{L}|)$, where n is the node number. We measure the empirical training speed and inference speed on an A100 server (Table 8). We can find that our high-order

Sentence & Analysis	Baseline	High-order
<p>#1: As well as previously (v1) holding senior positions at Barclays Bank (v2), BZW (v3) and Kleinwort Benson (v4), McCarthy was formerly a top civil servant at the Department of Trade and Industry.</p> <p>Analysis: Sibling factor helps our high-order model find the <i>BZW</i> which is tied for <i>Barclays Bank</i> to be an argument of event <i>Personnel:End-Position</i> triggered by word <i>previously</i>.</p>		
<p>#2: The crowd (v1) filled (v2) the street (v3) leading to the Kazimiya mosque in the northeast of Baghdad and carried banners in the green color of Islam, calling for good government.</p> <p>Analysis: An entity with <i>PER</i> type has less possibility to play an <i>Artifact</i> role. Ternary factor leverages messages passed by node label distributions to refine the edge label which in turn gives the message to refine node labels.</p>		

Figure 3: Examples showing how our high-order approach improves the graph prediction using different high-order factors. We only display a partial information graph for clearer illustration.

	FAC	GPE	LOC	ORG	PER
PER — PHYS → ?	-0.7183	-2.2627	0.4923	-0.6855	-6.1539
PER — PER-SOC → ?	-8.623	-6.1211	-8.1808	-4.54	18.0894
FAC — PART → ?	1.5584	-1.1251	-0.5099	0.2871	2.3058
GPE — PART → ?	-1.1251	0.6283	0.4069	-0.0478	-1.2592
LOC — WHOLE → ?	-0.5099	0.4069	1.5577	-2.1578	-0.613
ORG	0.2871	-0.0478	-2.1578	1.1853	-0.5345

PER: Person LOC: Location GPE: Geo-political entity
FAC: Facility ORG: Organization PHYS: Physical contains

Figure 4: Ternary scores between entity-relation-entity triples.

models are only slightly slower than the baseline despite the difference in computational complexity, which is because we implement our models with full GPU parallelization.

Visualization of Correlation Score We take relation extraction as an example to visualize the ternary score calculated by Eq. 3 between entity-relation-entity triples. For better understanding, we show examples of selected entity types and relation types. From Fig. 4, we can find that the correlation scores can reflect some prior knowledge. For example, ‘PER-SOC’ relation exists between two ‘PER’ entities, ‘PART-WHOLE’ relation is more likely to exist between entities with the same types.

Error Correction Analysis and Case Study

We provide quantitative error correction analysis in Appendix F. Figure 3 shows examples where our high-order approach revises wrong predictions made based on the initial unary scores (i.e., the first-order baseline), along with our analyses of how high-order factors achieve the revision.

4 Related Work

Classical IE models are typically task-specific (Lample et al., 2016b; Yu et al., 2020; Zeng et al., 2014; Wang et al., 2019a).

Recent efforts develop joint methods for two IE tasks (Miwa and Sasaki, 2014; Zheng et al., 2017; Nguyen and Nguyen, 2019; Zhang et al., 2019; Wang and Lu, 2020) or general architectures for universal IE (Paolini et al., 2021; Lu et al., 2022). These IE methods can roughly be divided into four schemes, namely, sequence labeling based (Lample et al., 2016b; Lin et al., 2019), sequence-to-structure based (Paolini et al., 2021; Lu et al., 2021b), generation based (Straková et al., 2019; Ma et al., 2019) and graph based (Fu et al., 2019; Sun et al., 2019; Luan et al., 2019a; Wadden et al., 2019; Lin et al., 2020a). This work is more relevant to the graph-based ones, which formulate IE as a graph prediction task that infers existences and labels of graph elements, i.e., nodes and edges. Wadden et al. (2019) use a dynamic span graph to enhance the expressiveness of graphic models. Fu et al. (2019) propose to use graph convolutional networks (GCNs) to jointly learn named entities and relations. Lin et al. (2020a) design a template to generate global features to help training. Different from these works, our approach designs a unified high-order inference scheme to jointly predict different variables.

5 Conclusion

In this paper, we propose a novel framework that leverages high-order interactions across different instances and different IE tasks in both training and inference processes. We formulate IE tasks as a unified graph prediction problem. Our framework consists of an identification module to identify spans as graph nodes and a classification module with high-order modeling and inference to jointly label all nodes and edges. Experimental results show that our high-order approach achieves consistent

improvement over previous work. The limitation of our work is that it is difficult to determine the best combination of different types of high-order factors. We take automatically selecting useful factors as our future work.

References

- Jacob Devlin, Ming-Wei Chang, Kenton Lee, and Kristina Toutanova. 2018. Bert: Pre-training of deep bidirectional transformers for language understanding. *arXiv preprint arXiv:1810.04805*.
- Rotem Dror, Segev Shlomov, and Roi Reichart. 2019. Deep dominance-how to properly compare deep neural models. In *Proceedings of the 57th Annual Meeting of the Association for Computational Linguistics*, pages 2773–2785.
- Rakesh Dugad and UDAY B Desai. 1996. A tutorial on hidden markov models. *Signal Processing and Artificial Neural Networks Laboratory, Dept of Electrical Engineering, Indian Institute of Technology, Bombay Technical Report No.: SPANN-96.1*.
- G David Forney. 1973. The viterbi algorithm. *Proceedings of the IEEE*, 61(3):268–278.
- Tsu-Jui Fu, Peng-Hsuan Li, and Wei-Yun Ma. 2019. GraphRel: Modeling text as relational graphs for joint entity and relation extraction. In *Proceedings of the 57th Annual Meeting of the Association for Computational Linguistics*, pages 1409–1418, Florence, Italy. Association for Computational Linguistics.
- Zixia Jia, Zhaohui Yan, Haoyi Wu, and Kewei Tu. 2022. Span-based semantic role labeling with argument pruning and second-order inference. In *Proceedings of the AAAI Conference on Artificial Intelligence*. AAAI Press.
- John Lafferty, Andrew McCallum, and Fernando CN Pereira. 2001. Conditional random fields: Probabilistic models for segmenting and labeling sequence data.
- Guillaume Lample, Miguel Ballesteros, Sandeep Subramanian, Kazuya Kawakami, and Chris Dyer. 2016a. Neural architectures for named entity recognition. *arXiv preprint arXiv:1603.01360*.
- Guillaume Lample, Miguel Ballesteros, Sandeep Subramanian, Kazuya Kawakami, and Chris Dyer. 2016b. Neural architectures for named entity recognition. In *Proceedings of the 2016 Conference of the North American Chapter of the Association for Computational Linguistics: Human Language Technologies*, pages 260–270, San Diego, California. Association for Computational Linguistics.
- Zhenzhong Lan, Mingda Chen, Sebastian Goodman, Kevin Gimpel, Piyush Sharma, and Radu Soricut. 2019. Albert: A lite bert for self-supervised learning of language representations. In *International Conference on Learning Representations*.
- Hongyu Lin, Yaojie Lu, Xianpei Han, and Le Sun. 2019. Sequence-to-nuggets: Nested entity mention detection via anchor-region networks. In *Proceedings of the 57th Annual Meeting of the Association for Computational Linguistics*, pages 5182–5192, Florence, Italy. Association for Computational Linguistics.
- Ying Lin, Heng Ji, Fei Huang, and Lingfei Wu. 2020a. A joint neural model for information extraction with global features. In *Proceedings of the 58th Annual Meeting of the Association for Computational Linguistics*, pages 7999–8009.
- Ying Lin, Heng Ji, Fei Huang, and Lingfei Wu. 2020b. A joint neural model for information extraction with global features. In *Proceedings of the 58th Annual Meeting of the Association for Computational Linguistics*, pages 7999–8009, Online. Association for Computational Linguistics.
- Xiao Liu, Heyan Huang, Ge Shi, and Bo Wang. 2022. Dynamic prefix-tuning for generative template-based event extraction. In *Proceedings of the 60th Annual Meeting of the Association for Computational Linguistics (Volume 1: Long Papers)*, pages 5216–5228, Dublin, Ireland. Association for Computational Linguistics.
- Chao Lou, Songlin Yang, and Kewei Tu. 2022. Nested named entity recognition as latent lexicalized constituency parsing. In *ACL*.
- Yaojie Lu, Hongyu Lin, Jin Xu, Xianpei Han, Jialong Tang, Annan Li, Le Sun, Meng Liao, and Shaoyi Chen. 2021a. Text2Event: Controllable sequence-to-structure generation for end-to-end event extraction. In *Proceedings of the 59th Annual Meeting of the Association for Computational Linguistics and the 11th International Joint Conference on Natural Language Processing (Volume 1: Long Papers)*, pages 2795–2806, Online. Association for Computational Linguistics.
- Yaojie Lu, Hongyu Lin, Jin Xu, Xianpei Han, Jialong Tang, Annan Li, Le Sun, Meng Liao, and Shaoyi Chen. 2021b. Text2event: Controllable sequence-to-structure generation for end-to-end event extraction. In *Proceedings of the 59th Annual Meeting of the Association for Computational Linguistics and the 11th International Joint Conference on Natural Language Processing (Volume 1: Long Papers)*, pages 2795–2806.
- Yaojie Lu, Qing Liu, Dai Dai, Xinyan Xiao, Hongyu Lin, Xianpei Han, Le Sun, and Hua Wu. 2022. Unified structure generation for universal information extraction. In *Proceedings of the 60th Annual Meeting of the Association for Computational Linguistics (Volume 1: Long Papers)*, pages 5755–5772.

- Yi Luan, Luheng He, Mari Ostendorf, and Hannaneh Hajishirzi. 2018. Multi-task identification of entities, relations, and coreference for scientific knowledge graph construction. *arXiv preprint arXiv:1808.09602*.
- Yi Luan, Dave Wadden, Luheng He, Amy Shah, Mari Ostendorf, and Hannaneh Hajishirzi. 2019a. A general framework for information extraction using dynamic span graphs. *arXiv preprint arXiv:1904.03296*.
- Yi Luan, Dave Wadden, Luheng He, Amy Shah, Mari Ostendorf, and Hannaneh Hajishirzi. 2019b. A general framework for information extraction using dynamic span graphs. In *Proceedings of the 2019 Conference of the North American Chapter of the Association for Computational Linguistics: Human Language Technologies, Volume 1 (Long and Short Papers)*, pages 3036–3046, Minneapolis, Minnesota. Association for Computational Linguistics.
- Dehong Ma, Sujian Li, Fangzhao Wu, Xing Xie, and Houfeng Wang. 2019. Exploring sequence-to-sequence learning in aspect term extraction. In *Proceedings of the 57th Annual Meeting of the Association for Computational Linguistics*, pages 3538–3547, Florence, Italy. Association for Computational Linguistics.
- Yubo Ma, Zehao Wang, Yixin Cao, Mukai Li, Meiqi Chen, Kun Wang, and Jing Shao. 2022. Prompt for extraction? PAIE: Prompting argument interaction for event argument extraction. In *Proceedings of the 60th Annual Meeting of the Association for Computational Linguistics (Volume 1: Long Papers)*, pages 6759–6774, Dublin, Ireland. Association for Computational Linguistics.
- Makoto Miwa and Yutaka Sasaki. 2014. Modeling joint entity and relation extraction with table representation. In *Proceedings of the 2014 Conference on Empirical Methods in Natural Language Processing, EMNLP 2014, October 25-29, 2014, Doha, Qatar; A meeting of SIGDAT, a Special Interest Group of the ACL*, pages 1858–1869. ACL.
- Trung Minh Nguyen and Thien Huu Nguyen. 2019. One for all: Neural joint modeling of entities and events. In *The Thirty-Third AAAI Conference on Artificial Intelligence, AAAI 2019, The Thirty-First Innovative Applications of Artificial Intelligence Conference, IAAI 2019, The Ninth AAAI Symposium on Educational Advances in Artificial Intelligence, EAAI 2019, Honolulu, Hawaii, USA, January 27 - February 1, 2019*, pages 6851–6858. AAAI Press.
- Giovanni Paolini, Ben Athiwaratkun, Jason Krone, Jie Ma, Alessandro Achille, Rishita Anubhai, Cicero Nogueira dos Santos, Bing Xiang, and Stefano Soatto. 2021. Structured prediction as translation between augmented natural languages. In *9th International Conference on Learning Representations, ICLR 2021, Virtual Event, Austria, May 3-7, 2021*. OpenReview.net.
- Jana Straková, Milan Straka, and Jan Hajic. 2019. Neural architectures for nested NER through linearization. In *Proceedings of the 57th Annual Meeting of the Association for Computational Linguistics*, pages 5326–5331, Florence, Italy. Association for Computational Linguistics.
- Changzhi Sun, Yeyun Gong, Yuanbin Wu, Ming Gong, Daxin Jiang, Man Lan, Shiliang Sun, and Nan Duan. 2019. Joint type inference on entities and relations via graph convolutional networks. In *Proceedings of the 57th Annual Meeting of the Association for Computational Linguistics*, pages 1361–1370, Florence, Italy. Association for Computational Linguistics.
- David Wadden, Ulme Wennberg, Yi Luan, and Hannaneh Hajishirzi. 2019. Entity, relation, and event extraction with contextualized span representations. In *Proceedings of the 2019 Conference on Empirical Methods in Natural Language Processing and the 9th International Joint Conference on Natural Language Processing (EMNLP-IJCNLP)*, pages 5784–5789, Hong Kong, China. Association for Computational Linguistics.
- Christopher Walker, Stephanie Strassel, Medero Julie, and Kazuaki Maeda. 2005. Ace 2005 multilingual training corpus.
- Haoyu Wang, Ming Tan, Mo Yu, Shiyu Chang, Dakuo Wang, Kun Xu, Xiaoxiao Guo, and Saloni Potdar. 2019a. Extracting multiple-relations in one-pass with pre-trained transformers. In *Proceedings of the 57th Annual Meeting of the Association for Computational Linguistics*, pages 1371–1377, Florence, Italy. Association for Computational Linguistics.
- Jue Wang and Wei Lu. 2020. Two are better than one: Joint entity and relation extraction with table-sequence encoders. In *Proceedings of the 2020 Conference on Empirical Methods in Natural Language Processing (EMNLP)*, pages 1706–1721, Online. Association for Computational Linguistics.
- Wenya Wang and Sinno Jialin Pan. 2020. Integrating deep learning with logic fusion for information extraction. In *Proceedings of the AAAI Conference on Artificial Intelligence*, volume 34, pages 9225–9232.
- Wenya Wang and Sinno Jialin Pan. 2021. Variational deep logic network for joint inference of entities and relations. *Computational Linguistics*, pages 1–38.
- Xinyu Wang, Jingxian Huang, and Kewei Tu. 2019b. Second-order semantic dependency parsing with end-to-end neural networks. *arXiv preprint arXiv:1906.07880*.
- Xinyu Wang and Kewei Tu. 2020. Second-order neural dependency parsing with message passing and end-to-end training. *arXiv preprint arXiv:2010.05003*.
- Yijun Wang, Changzhi Sun, Yuanbin Wu, Hao Zhou, Lei Li, and Junchi Yan. 2021. Unire: A unified label space for entity relation extraction. In *Proceedings of the 59th Annual Meeting of the Association*

for *Computational Linguistics and the 11th International Joint Conference on Natural Language Processing (Volume 1: Long Papers)*, pages 220–231.

Eric P Xing, Michael I Jordan, and Stuart Russell. 2012. A generalized mean field algorithm for variational inference in exponential families. *arXiv preprint arXiv:1212.2512*.

Zhiheng Yan, Chong Zhang, Jinlan Fu, Qi Zhang, and Zhongyu Wei. 2021. [A partition filter network for joint entity and relation extraction](#). In *Proceedings of the 2021 Conference on Empirical Methods in Natural Language Processing, EMNLP 2021, Virtual Event / Punta Cana, Dominican Republic, 7-11 November, 2021*, pages 185–197. Association for Computational Linguistics.

Deming Ye, Yankai Lin, Peng Li, and Maosong Sun. 2022. Packed levitated marker for entity and relation extraction. In *Proceedings of the 60th Annual Meeting of the Association for Computational Linguistics (Volume 1: Long Papers)*, pages 4904–4917.

Juntao Yu, Bernd Bohnet, and Massimo Poesio. 2020. [Named entity recognition as dependency parsing](#). In *Proceedings of the 58th Annual Meeting of the Association for Computational Linguistics*, pages 6470–6476, Online. Association for Computational Linguistics.

Daojian Zeng, Kang Liu, Siwei Lai, Guangyou Zhou, and Jun Zhao. 2014. [Relation classification via convolutional deep neural network](#). In *Proceedings of COLING 2014, the 25th International Conference on Computational Linguistics: Technical Papers*, pages 2335–2344, Dublin, Ireland. Dublin City University and Association for Computational Linguistics.

Tongtao Zhang, Heng Ji, and Avirup Sil. 2019. [Joint entity and event extraction with generative adversarial imitation learning](#). *Data Intell.*, 1(2):99–120.

Shuai Zheng, Sadeep Jayasumana, Bernardino Romera-Paredes, Vibhav Vineet, Zhizhong Su, Dalong Du, Chang Huang, and Philip HS Torr. 2015. Conditional random fields as recurrent neural networks. In *Proceedings of the IEEE international conference on computer vision*, pages 1529–1537.

Suncong Zheng, Feng Wang, Hongyun Bao, Yuexing Hao, Peng Zhou, and Bo Xu. 2017. [Joint extraction of entities and relations based on a novel tagging scheme](#). In *Proceedings of the 55th Annual Meeting of the Association for Computational Linguistics, ACL 2017, Vancouver, Canada, July 30 - August 4, Volume 1: Long Papers*, pages 1227–1236. Association for Computational Linguistics.

Zexuan Zhong and Danqi Chen. 2020. A frustratingly easy approach for entity and relation extraction. *arXiv preprint arXiv:2010.12812*.

A Details on Identification Module

A multi-layer perceptron (MLP) takes word representations $H = [\mathbf{h}_1, \dots, \mathbf{h}_n]$ as input and outputs an emission score \mathbf{u}_i for each word. With a learnable transition score matrix A , a labeled sequence $\mathbf{y} = (y_1, \dots, y_n)$ can be scored as $s(\mathbf{y}, H) = \sum_{i=1}^n (\mathbf{u}_i)_{y_i} + A_{y_{i-1}, y_i}$.

Inference We use the Viterbi algorithm (Forney, 1973) to obtain the sequence that has the highest score: $\hat{\mathbf{y}} = \arg \max_{\mathbf{y}} s(\mathbf{y}, H)$.

Learning We maximize the probability of the target sequence to learn the identification module.

$$P(\mathbf{y}^* | \mathbf{w}) = \frac{\exp(s(\mathbf{y}^*, H))}{\sum_{\mathbf{y}'} \exp(s(\mathbf{y}', H))} = \frac{1}{\mathcal{Z}} \exp(s(\mathbf{y}^*, H))$$

where \mathbf{y}^* is the target sequence and \mathcal{Z} is the partition function. We can use the forward-backward algorithm (Dugad and Desai, 1996) to calculate \mathcal{Z} .

Of note, we did not consider nested spans in this work, which can easily be adopted to our framework using similar methods as in Yu et al. (2020); Lou et al. (2022) to identify graph nodes if span nesting.

B Dataset Statistics

Statistics of all datasets we used are shown in Table 9.

	Split	#Sentences	#Entities	#Relations	#Events
ACE05-R	Train	10,051	26,473	4,788	-
	Dev	2,424	6,362	1,131	-
	Test	2,050	5,476	1,151	-
ACE05-E	Train	17,172	29,006	4,664	4,202
	Dev	923	2,451	560	450
	Test	832	3,017	636	403
ACE05-E+	Train	19,216	47,525	7,152	4,419
	Dev	902	3,422	728	468
	Test	676	3,673	802	424
ACE05-CN	Train	6841	29657	7934	2926
	Dev	526	2250	596	217
	Test	547	2388	672	190

Table 9: Datasets statistics

C Hyper-parameters

For the hidden sizes of unary FNNs and most optimizer parameters, we use the default hyper-parameters following (Lin et al., 2020a). The hidden sizes of FNNs in high-order scoring are tuned between $\{150, 300\}$. The iteration step T of MFVI is tuned between $\{1, 2, 3\}$, and it is set to 1 or 2 in different settings. We choose the hyper-parameters

according to the performance of the development set after 80 epoch runs. The main hyper-parameters are listed in Table 10.

Setting	Value
Unary scoring	
FNN(entity)	150
FNN(trigger)	600
FNN(relation)	150
FNN(role)	600
Binary scoring	
FNN(head)	150
FNN(tail)	150
FNN(mid)	150
Ternary scoring	
FNN(head)	150
FNN(tail)	150
Other setting	
batch size	10
dropout rate	0.4
learning rate of Pretrained LM encoder	1e-5
lr decay of Pretrained LM encoder	1e-5
learning rate of other modules	1e-3
lr decay of other modules	1e-3
warm-up epochs	5
total epochs	80
gradient clipping	5.0

Table 10: Summary of hyper-parameters

D Re-evaluation of PL-Marker

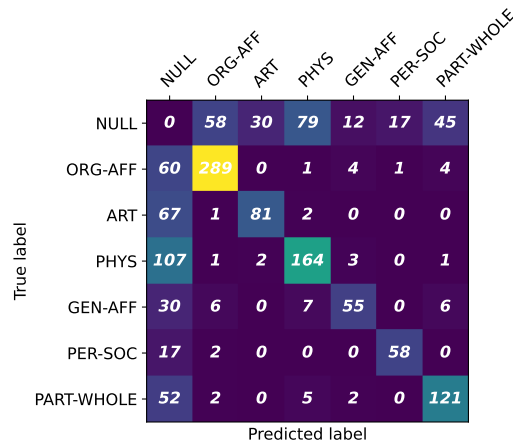
For the relation extraction task, some corpus have symmetric relations, meaning the ordering of the two entities does not matter (e.g., ‘PER-SOC’ in ACE2005). A symmetric relation is only annotated in one direction in the annotation data. PL-Marker counts a symmetric relation twice both for prediction number and gold number, but other work only counts once for the prediction and gold numbers.

E Experimental results on ACE05-E+

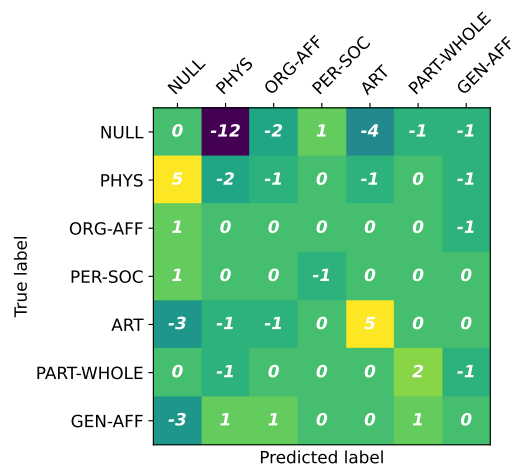
Table 11 shows the experimental results of three settings with sibling factor: *role-sib* representing sib of role pairs, *rel-sib* representing sib of relation pairs, and *r+r-sib* representing sib of both role pairs and relation pairs.

F Error Correction Analysis

We take joint EntR and ReE as an example to show the number of error corrections of our high-order model compared to our baseline model in terms of relation types. From Fig. 5, we can find that our high-order model corrects the errors of our baseline model in relation types (the numbers are expected to be positive in the diagonal and to be negative otherwise).



(a) Our baseline



(b) Error correction matrix

Figure 5: Confusion matrix of the relation types. (a) The relation numbers of our baseline model on predicted entities. (b) The correction numbers of our high-order model relative to the baseline model. We do not have statistics on Null-Null.

Sentence & Analysis	Baseline	High-order
<p>#1: As well as previously (v1) holding senior positions at Barclays Bank (v2), BZW (v3) and Kleinwort Benson (v4), McCarthy was formerly a top civil servant at the Department of Trade and Industry.</p> <p>Analysis: Sibling factor helps our high-order model find the <i>BZW</i> which is tied for <i>Barclays Bank</i> to be an argument of event <i>Personnel:End-Position</i> triggered by word <i>previously</i>.</p>		
<p>#2: The crowd (v1) filled (v2) the street (v3) leading to the Kazimiya mosque in the northeast of Baghdad and carried banners in the green color of Islam, calling for good government.</p> <p>Analysis: An entity with <i>PER</i> type has less possibility to play an <i>Artifact</i> role. Ternary factor leverages messages passed by node label distributions to refine the edge label which in turn gives the message to refine node labels.</p>		
<p>#3: For the most part the marches went off peacefully, but in New York (v1) a small group (v2) of protesters were arrested after they refused to go home (v3) at the end of their rally, police sources said.</p> <p>Analysis: There is less possibility that a <i>PER</i> entity has <i>PHYS</i> relation with <i>GPE</i> entity and <i>FAC</i> entity at the same time. Sibling and ternary factors help our high-order model in this situation.</p>		

Figure 6: Examples showing how our high-order approach improves the graph prediction using different high-order factors. We only display a partial information graph for clearer illustration.

	Ent	Rel	Tri-I	Tri-C	Arg-I	Arg-C
Our baseline	90.8	65.3	77.4	74.6	60.0	58.1
Our <i>homo</i> (role-sib)	90.8	65.1	77.4	74.6	60.3	58.4
Our <i>homo</i> (rel-sib)	91.0	65.6	77.4	74.8	60.1	58.5
Our <i>homo</i> (r+r-sib)	90.9	65.4	77.4	74.8	60.1	58.3

Table 11: Average F1 on ACE05-E+ dataset.

G More Case Study

We show more cases in Fig. 6.

H More Related Work

High-order Methods Previous high-order methods most focus on instance interactions in training process to get more expressive representations, such as sharing representations (Sun et al., 2019; Luan et al., 2019b) or using sequence-to-sequence architecture (Ma et al., 2022; Paolini et al., 2021; Lu et al., 2021b). There are some high-order inference methods that are related to us on different NLP tasks. On dependency parsing, Wang and Tu (2020) considered three types of second-order parts of semantic dependencies and approximate decoding with mean-field variational inference or loopy belief propagation. Jia et al. (2022) considered interactions between two arguments of the same predicate on semantic role labeling task. However, due to the complexity, they only did high-order inference on edge existence prediction while leaving label prediction in first-order, and they did not involve heterogeneous factors. In another line of research, Wang and Pan (2020, 2021) integrate logic

rules and neural network to leverage prior knowledge to help relation extraction and event extraction tasks. But they cannot achieve end-to-end training and inference.

I Limitations

The first limitation is caused by the high complexity of high-order inference. As analysed in Section 3.2, the complexity of our approach is related to the node number of a graph. Thus we firstly identify the nodes with a separate module, which can cause error propagation. Taking joint node identification and label classification with high-order inference into account should enumerate all possible spans in a sentence, which is too computationally expensive. A possible solution is that we use pruning to decrease the number of possible spans and use some decomposition methods to decrease the computation complexity of inference. We take joint node identification and label classification with high-order inference as future work.

The second limitation is the difficulty to determine the combination of different types of high-order factors. From our experimental results, we found that compared with leveraging a single factor, leveraging multiple factors only slightly improved the performance. The reason may be that messages from different types of factors may conflict with each other, such that training becomes more difficult. Thus how to automatically select the useful factors or control the scale of messages passed by different factors is a meaningful research direction

in future work.